Geometric dependence of 3D collective cancer invasion

Jihan Kim*,[1] Yu Zheng*,[2] Amani A. Alobaidi*,[1] Hanqing Nan,[3] Jianxiang Tian,[4,3] Yang Jiao,[3,2,†] and Bo Sun[1,‡]

[1]*Department of Physics, Oregon State University, 301 Weniger Hall, Corvallis, OR, USA, 97331-6507*
[2]*Department of Physics, Arizona State University, Tempe, AZ 85287-6106*
[3]*Materials Science and Engineering, Arizona State University, Tempe, AZ 85287-6106*
[4]*Department of Physics, Qufu Normal University, Qufu 273165, China*

Metastasis of mesenchymal tumor cells is traditionally considered as a single cell process. Here we report an emergent collective phenomenon where the dissemination rate of mesenchymal breast cancer cells from 3D tumors depends on the tumor geometry. Combining experimental measurements and computational modeling we demonstrate that the collective dynamics is coordinated by the mechanical feedback between individual cells and their surrounding extracellular matrix (ECM). We find the tissue-like fibrous ECM supports long-range physical interactions between cells, which turn geometric cues into regulated cell dissemination dynamics. Our results suggest that migrating cells in 3D ECM represent a distinct class of active particle system where the collective dynamics is governed by remodeling of the environment rather than direct particle-particle interactions.

Statement of Significance

Collective migration of cells are of enormous interests to both physical and biomedical sciences. Previous studies of collective cell migration have almost exclusively focused on 2D systems where direct cell-cell interactions are important. Here we report collective cancer invasion in 3D extracellular matrix (ECM), where coordinated dynamics emerges from novel mechanism involving cell-ECM micro-mechanical interactions, leading to geometry-dependent rate of cancer cell dissemination from tumors. Our results demonstrate on a fundamental level how novel collective cell dynamics can arise from indirect interactions, and depend on reconfigurability of the environment. This opens up many future research directions in the physics of active particles, micro-mechanics of cell-ECM systems and collective dynamics of cancer metastasis.

Introduction

Metastasis of tumors, particularly carcinomas, is traditionally considered to be a single cell process following the epithelial-mesenchymal-transition [1]. However, recent observations suggest that even mesenchymal tumor cells – cells that have lost E-cadherin adhesions with each other – coordinate their invasion dynamics. Such coordination can be achieved by exchange of diffusive factors that establish leader-follower phenotypes [2]; or through microtracks in the tissue that confine cells into single file strands [3, 4]. These observations highlight the diverse modes of cancer invasion, and open new targets to interfere the lethal metastasis of tumors [5, 6].

In this paper, we report a surprising observation that dissemination rate of mesenchymal cancer cells from a tumor depend on the tumor geometry. The geometric dependence, as we show experimentally and computationally, is a result of collective extracellular matrix (ECM) remodeling by the tumor cells. In particular, cell-generated forces coupled with the mechanical reconfigurability of the ECM create physical cues that are modulated by tumor geometry to bias individual cell migration. Our results suggest that ECM-mediated physical interactions between cancer cells play a powerful role in determining the metastatic potential of malignant tumors.

Results

Geometry controls tumor invasiveness and modulates collective ECM remodeling

To study the collective invasion of solid tumors, we use *in vitro* tumor models in 3D cultures, which offer more physiologically relevant insights compared with 2D assays [7]. We create model tumors as cancer cell clusters with our DIGME technique [8]. Each tumor consists of approximately 1000 GFP-labeled, highly invasive mensenchymal breast cancer cells MDA-MB-231 molded into various shapes in 3D collagen ECM (Fig. S1). The tumors typically have thickness of 2-3 layers of cells [8, 9], which allows us to image through the whole tumors. Confocal imaging starts immediately after the gelation process completes (time zero).

We first compare tumors of two different cross-sectional geometries: circular and triangular. In particular, we measure the invasion depths Δd as the distance between the outer boundaries of the tumors at day 0 and day 10 as shown in Fig. 1(a-b). The circular tumors disseminate rapidly, with the mean invasion depth

*These authors contributed equally to this work.
†correspondence sent to: yang.jiao.2@asu.edu
‡correspondence sent to: sunb@onid.orst.edu

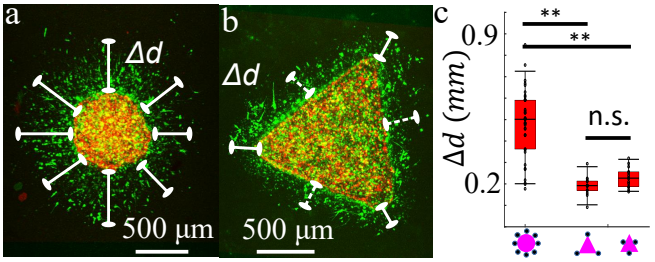

FIG. 1: Geometry controls tumor invasiveness. (a-b) Tumor morphology shown by maximum projection at day 0 (red) and day 10 (green). For a circular tumor the invasion depth Δd is measured along eight equally spaced angles (a). For a triangular tumor Δd is measured along tip and edge directions separately (b). (c) The invasion depths of circular and triangular tumors. N =5 tumors were measured for each geometry. Statistical comparison are done with t-test. **: p<0.01. n. s. : not significant.

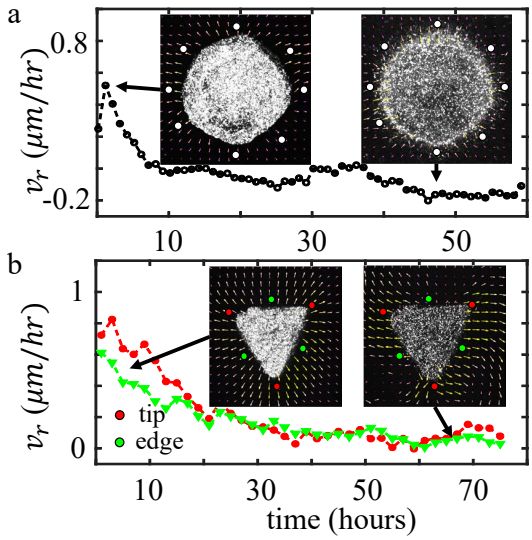

FIG. 2: Geometry controls ECM remodeling by tumors. (a-b) The average radial velocity of the ECM deformation near expanding tumors. In (a) the velocity is averaged over the 8 dotted locations shown in the inset. In (b) the velocity is averaged over the dotted locations along the edge and tip directions respectively. Insets show the net deformation of the ECM at two time points (black arrows).

to be more than 500 μm. The triangular tumors, on the other hand, disseminate much slower. The invasion depths measured in the edge and tip directions are both around 200 μm, less than half of the mean invasion depth of circular tumors (Fig. 1c).

We note that there are rarely any cell-cell adhesions or cell strands during the invasion process, which is consistent with the highly mesenchymal nature of MDA-MB-231 cells. The geometry-dependent invasiveness is also not attributable to genetic or phenotypical differences as the cells are harvested from the same culture source.

We then consider the possibility of ECM-mediated indirect cell-cell interactions. Previously we reported that the traction forces from cell pairs create aligned collagen fiber bundles, such that the remodeled ECM provides a potential channel to mediate mechanical communications between cancer cells [10]. For a disseminating tumor, the micromechanical remodeling of the ECM could be even stronger due to additive effects. Therefore, we hypothesize that collective cell remodeling of the ECM renders the invasion of a tumor to depend on its geometry.

To test this hypothesis, we first examine if the ECM deformation caused by tumor-generated forces depends on the tumor geometry. We embed 1-μm diameter fluorescent polystyrene particles in the collagen ECM and use particle image velocimetry (PIV) to quantify the ECM deformation field. Fig. 2 (a-b) show the radial velocity v_r of the ECM by averaging over symmetric locations (dotted points in the insets). A circular tumor first pushes out the ECM ($v_r > 0$) due to cell spreading upon seeding (leading to overall expansion of the tumor, see Fig. S2), then pulls in the ECM ($v_r < 0$) with their traction force. As a result, after 2 days the ECM shows net inward deformation while some of the cells have already disseminated from the tumor (Fig. 2a insets). On the other hand, we find that a triangular tumor mostly pushes out the ECM, albeit with a diminishing rate. As a result, the ECM surrounding the triangular tumor maintains a radially outward net deformation (Fig. 2b).

Computational modeling demonstrates geometric dependence of tumor invasiveness

To further test our hypothesis in explaining the observed contrast between circular and triangular tumors, we devise a multi-scale computational model that takes into account the fibrous microstructure of the ECM [11, 12], nonlinear ECM mechanics [13–15], as well as cell motility directed by ECM mechanical cues [16–19]. In particular, in our simulations, the tumor diskoid is modeled as a 3D packing of (spherical) cells within a flat cylinder with a thickness of 100 microns (i.e., about 4 to 5 cell length) (see Fig. S7). We use realistic 3D geometry and 3D micro-mechanics in modeling the invasion and migration of the tumor cells in the ECM (see Fig. S6). To be consistent with the experiments, we only keep track of the dynamics of the cells in the x-y plane. The underlying assumption is that cell migration in the z-direction is independent of xy-plane motility. The details of the computational models are provided in the Supporting Information file.

Based on the experimental observations, we consider the dissemination of tumor to start from an expansion phase, where cells spread and push out the ECM. This is followed by an invasion phase, where cells pull in the ECM and migrate. We model tumor cells as polarized active particles with coupled force generation and locomotion [16] (Fig. S3-S8). Cells deform the ECM fibers in their vicinity, which in turn alters the migration and polarization of the cells. Explicitly accounting for the

reciprocal interactions between cells and ECM allows us to investigate the collective migration regulated by the non-local mechanical dialogues among the cells mediated by the ECM.

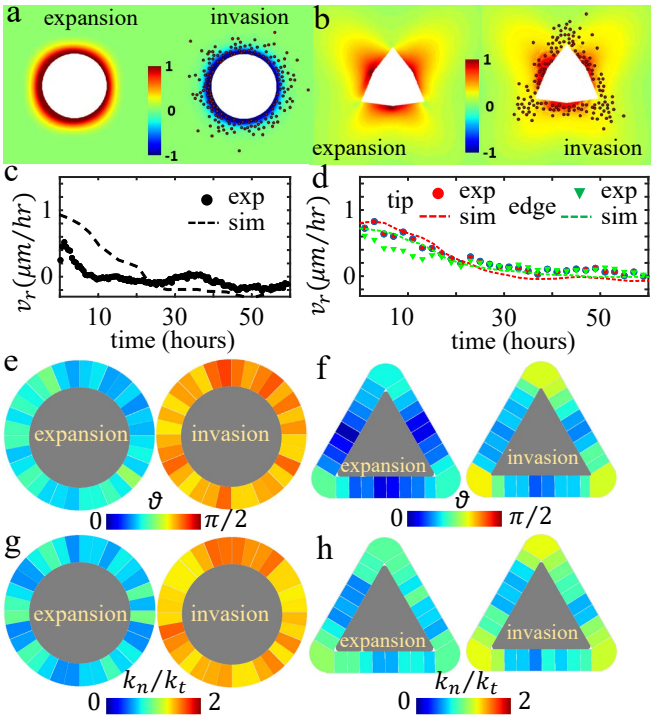

FIG. 3: Simulated ECM remodeling by circular and triangular tumors. (a-b) The radial displacement of ECM at 5 hours (representing the expansion phase) and at 50 hours (representing invasion phase) of circular and triangular tumors. Maximum magnitude of deformation is normalized to 1. (c-d) Radial velocities of the ECM sampled near circular and triangular tumors at locations corresponding to the experimental measurements in Fig. 1(e-f). Abbreviations: exp: experiment; sim: simulation. (e-f) The orientation of ECM fibers near the tumors at 5 hours (expansion) and at 50 hours (invasion). θ is measured as the average angle of fibers with respect to their local tangential direction of the tumor boundary. (e-f) The micromechanical anisotropy defined as k_n/k_t at 5 hours (expansion) and at 50 hours (invasion). k_n and k_t are the micromechanical stiffness along the normal direction and tangential direction of the tumor boundary respectively. See Fig. S8 for more details. In (e-h) we sample 100 μm^3 volume elements next to the tumors to obtain the average fiber orientations and stiffness ratios.

We first employ the computational model to simulate and calculate the remodeling of the ECM surrounding circular and triangular tumors. Fig. 3 (a-b) show the relative magnitudes of displacement fields in the ECM, where the maximum value is normalized to 1. Here we measure the ECM properties at 5 hours and 50 hours, two time points empirically determined to represent the expansion and invasion phases respectively. The magnitude of displacement decays roughly as $1/r^3$ as one moves away from the tumors. After the expansion phase, individual cells migrate away from the original tumor. The right panels of Fig. 3(a-b) show locations of the invaded cells in a typical simulation run. Cell invasion is accompanied with continuous ECM deformation. As shown in Fig. 3(c-d), our simulated ECM radial velocity agree well (qualitatively for circular tumors and quantitatively for triangular tumors) with experimental measurements. Importantly, the contractile deformation is much more pronounced near circular tumors compared with triangular tumors.

We note that compressive deformation in the ECM due to the initial expansion of the tumor predicted in the simulations is larger than that measured experimentally (see Fig. 3(c)). We speculate that main reason for this discrepancy is that in our simulations, we did not explicitly model the plasticity of the ECM fibers. It is reasonable to expect that the ECM at the tumor edge, which is subject to large compressive stress due to the expanding tumor, is in the plastic regime. This would reduce the compressive stress in ECM further away from the tumor, leading to reduced deformation field in these regions (where the deformations are measured).

To better reveal the structural remodeling of the ECM, we have calculated the average orientation of the ECM fibers with respect to the tangential direction of the tumor surfaces (Fig. 3e-f). During the expansion phase, tumors push the fibers to be aligned parallel to the tumor boundary, which bias the cell polarization accordingly. Later on, the pulling forces from the cells reorient the fibers. For circular tumors, the collective cellular traction force is sufficient to align the ECM fibers radially (Fig. 3e), contributing to the accelerated the dissemination. In contrast, the fibers remain tangentially aligned along the flat edges of the triangular tumors (Fig. 3f).

The structural remodeling of the ECM significantly reconfigures the micromechanics of the ECM. We find that for both circular and triangular tumors ECM is consistently stiffer in the direction of fiber alignment, and softer in the direction perpendicular to the fibers. Such mechanical cues may further regulate the dynamics and functions of cells through mechanosensing pathways [20].

Our simulations show that the circular tumors exhibit larger invasion depths compared with the triangular tumors (Fig. S10), which is consistent with the experimental observations. To further explore the mechanisms behind the geometry-dependent collective migration, we modified the simulation parameters to steer the cell-ECM interactions. We find that when the cell polarization and ECM fiber orientations become uncorrelated, the invasion depth of tumors drastically reduces (Fig. S11). This is consistent with the experimental results that reducing the level of contact guidance diminished the advantage of circular tumors in dissemination (Fig. S12). We also find that reducing the cellular traction forces leads to weaker ECM remodeling, and thus weaker dependence of tumor invasion dynamics on the tumor geometry (Fig. S13).

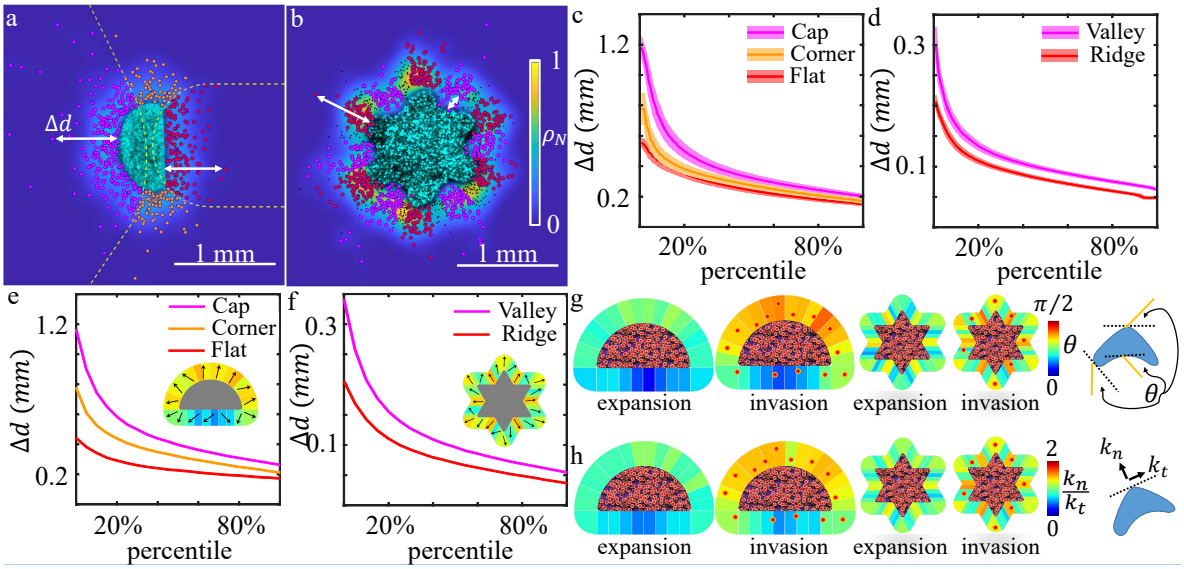

FIG. 4: Collective invasion of tumor cells with complex shapes. (a-b) Snapshots of semicircular and star-shaped diskoids at day 10 and day 3 respectively. The images of the tumors at day zero are surrounded by the normalized cell density ρ_N (see text). Dots represent locations of all the disseminated cells experimentally observed for each tumor shape. In (a) the ECM space is divided into cap, corner and flat regions separated by the yellow dashed curves. In (b) the ECM space is divided into ridge and valley regions. Cells in different regions are labeled with different colors. The invasion depth Δd of a cell is the distance between the cell and the boundary of the tumor at day zero (white arrows show examples). (c-d) Ranked average invasion depths (RAID) of semicircular and star-shaped diskoids. The solid lines and shaded areas represent the means and standard deviations obtained from 500 bootstraps. In (a-d) approximately 1000 disseminated cells are identified and included in the statistics from N=4 (semicircular diskoid) and N = 5 (star diskoid) biological replicas respectively. (e-f) Simulated RAID profiles for semicircular and star shaped tumors. Insets: magnitude (heat map, normalized by maximum), and direction (arrows) of average cell velocity near the tumors. (g-h) The simulated average fiber orientation and micromechanical anisotropy in a layer of $\sim 100\mu m$ surrounding the tumors after the expansion and invasion phases. Here θ is defined as the acute angle between a fiber and the local tangential direction of the tumor boundary, while k_n and k_t are defined previously (Fig. S9). One simulation (i.e., N = 1) is performed for each geometry.

Invasion characteristics of tumors with complex geometries

Having tested our simulation model against experimental results for circular and triangular tumors, we ask if the mechanical principles considered in our model are sufficient to predict the invasiveness of tumors with more complex geometries. We focus on two particular shapes of tumors: semicircle and star. The boundary of a semicircle contains regions of both positive and zero curvature, therefore can be considered to be a hybrid of circular and triangular tumors. A star shape, on the other hand, contains both convex and concave surfaces.

Taking into account of the asymmetric shape of semicircular diskoids, we divide the ECM space into cap, corner and flat regions (Fig. 4a). We manually identify all disseminated cells and their locations $\mathbf{r}_i$ after 10 days from seeding the original tumor. We compute the normalized cell density $\rho_N(\mathbf{r}) = \frac{A_0}{m}\sum_{i=1}^{m}\frac{1}{2\pi\sigma^2}e^{-\frac{(\mathbf{r}-\mathbf{r}_i)^2}{2\sigma^2}}$, where m is the total number of disseminated cells, A_0 is the area of the original tumor diskoid and kernel width $\sigma = 80\mu$m, is approximately twice the size of a cell. ρ_N represents a dilution factor: if $\rho_N = 1$ then the local cell density is the same as in the original tumor, where all cells are presumably uniformly distributed.

We find the cell density is almost uniform surrounding the semicircular diskoid, and decreases rapidly at larger distance. However, the flat region contains fewer cells that migrate deeply into the ECM space from the diskoid boundary. To further quantify the relation between invasiveness and local geometry of tumors, we calculate the ranked average invasion depths (RAID) $\Delta\bar{D}(f)$. In particular, we first measure the invasion depth Δd_i of each cell i as the distance of the cell from the original tumor boundary (arrows in Fig. 4a,b). We then compute $\Delta\bar{D}(f)$ as the average invasion depth of cells in the top f percentile ranked by Δd_i. Using the metric RAID, we compare the invasiveness of cells in each of the three regions of the ECM surrounding semicircular diskoids. As shown in Figure. 4c, cells in the cap region are leading the dissemination. For instance, the top 10% invaders in the cap region have an average invasion depth of 672 μm, while the top 10% invaders in the corner and flat region have an average invasion depth of 470 μm. At a percentile of 5%, cells in the cap region have a lead of 200 μm than cells in the flat region.

Consistent with the previous observations in Fig. 1,

the invasiveness of semicircular diskoids provides strong evidence that local geometry regulates cancer cell dissemination. In particular, a positive curvature in the tumor surface accelerates the overall invasion [21].

We have also quantified the invasiveness of star-shaped diskoids after 3 days of seeding the tumor. In particular, we divide the ECM space into regions that are in the direction of the tips (positive curvature), and regions that are in the direction of valleys (negative curvature). Cells in the buffer regions (black dots in Fig. 4b) are excluded from the analysis.

By measuring RAID we find that overall cells in the valley region possess larger invasion depth (Fig. 4d), suggesting that negative curvature accelerates cell dissemination even more than positive curvature. Of note, at 10 days, the disseminated cells become uniformly distributed in all directions. This is due to the proximity of the ridge and valley regions as well as the mixing caused by lateral motion of the cells,

These experimental results agree well with the predictions of our simulations as shown in Fig. 4e and f. Furthermore, our simulations also reveal the ECM remodeling by the tumors. Fig. 4(g-h) shows the average fiber orientation and microscopic anisotropy in the expansion and invasion phases. For semicircular tumors, fibers in the flat region remain tangentially aligned to the tumor boundary through the whole process; whereas fibers in the cap region are re-oriented radially by cellular traction force during the invasion phase. For star-shaped tumors, fiber orientation in the ridge region rotates from tangential of the tumor boundary to random alignment; whereas fibers in the valley region are pulled normal to the tumor boundary during the invasion phase. The structual anisotropy translates directly to the micromechanical anisotropy, such that the ECM is stiffer in the direction parallel to the fiber alignment. These results confirm that local geometry program collective force generation and ECM remodeling by the cancer cells, which modulates the rate of dissemination of the tumors.

Conclusion and discussion

In this paper, we show that tumor geometry modulates the 3D invasion potential of a tumor. We find that the geometric dependence is due to a physical mechanism that depends on the bi-directional interaction between individual cells and the ECM surrounding a tumor. This mechanism does not require direct contact between cells such as cadherin-based adhesion [22, 23] or contact inhibition [24, 25], nor does it rely on the cooperation of leader-follower phenotypes [3, 4, 26, 27]. Instead, we show both experimentally and computationally that cells collectively apply forces to their ECM [28], which in turn provides geometric dependent mechanical cues to bias 3D cell motility and dissemination.

We note that recent studies [29, 30] have suggested that the initiation of cancer cell dissemination can be considered as a jamming to unjamming transition, depending on the energy barrier associated with local cell re-arrangement, which in turn systematically depends on the number of neighbors of a cell. While our work focuses more on the subsequent invasion dynamics, and the micromechanical interactions between tumor cells and the ECM, it will be interesting to investigate how tumor geometry, and the coupling with ECM modulate the jamming-unjamming transitions.

Our results provide physical insights for processes in cancer biology and morphogenesis. Clinical studies have shown that collagen fibers aligned tangentially and normally to tumor boundary correspond to opposite prognosis [31, 32]. While the origin of tumor-associated ECM misalignment is unclear, our results suggest that tumor geometry may be an important contributing factor. On the other hand, mesenchymal cell migration is often considered as a single-cell process during development and diseases [1, 33]. Our model system show that underlying multicellular coordination may take place in the form of collective force generation and ECM remodeling. Together, we find that 3D collective cell migration may exploit the mechanical feedback between force-generating cells and reconfigurable ECM as an indirect yet effective channel of communication .

Finally, our results show that 3D migrating cells represent a distinct class of active particles which actively re-sculpture their microenvironment and respond to the cues generated by themselves and others. Future research is needed to systematically investigate the collective dynamics of such active particles as a route to understand general living systems.

Data Availability

All data and computer codes are available from the authors upon reasonable request.

Acknowledgment

The research is supported by a Scialog Program sponsored jointly by Research Corporation for Science Advancement and the Gordon and Betty Moore Foundation through a grant to Oregon State University by the Gordon and Betty Moore Foundation. B. S. is partially supported by the Medical Research Foundation of Oregon and SciRIS-II award from Oregon State University. J. K. is partially supported by the National Science Foundation grant PHY-1400968. Y. Z. and Y. J. are partially supoorted by the National Science Foundation grant CMMI-1916878.

Author Contributions

B. S. and Y. J. designed the research and oversaw the experimental and computational studies respectively. J. K., Y. Z., A. A., H. N., J. T. collected data. All authors analyzed data and wrote the manuscript.

[1] Jonathan M Lee, Shoukat Dedhar, Raghu Kalluri, and Erik W Thompson. The epithelial-mesenchymal transition: new insights in signaling, development, and disease. *The Journal of cell biology*, 172(7):973–81, 2006.

[2] J Konen, E Summerbell, B Dwivedi, K Galior, Y Hou, L Rusnak, A Chen, J Saltz, W Zhou, L H Boise, P Vertino, L Cooper, K Salaita, J Kowalski, and A I Marcus. Image-guided genomics of phenotypically heterogeneous populations reveals vascular signalling during symbiotic collective cancer invasion. *Nat. Comm.*, 8:15078, 2017.

[3] Katarina Wolf, Yi I. Wu, Yueying Liu, Jörg Geiger, Eric Tam, Christopher Overall, M. Sharon Stack, and Peter Friedl. Multi-step pericellular proteolysis controls the transition from individual to collective cancer cell invasion. *Nature Cell Biology*, 9(8):893–904, 2007.

[4] Cedric Gaggioli, Steven Hooper, Cristina Hidalgo-Carcedo, Robert Grosse, John F. Marshall, Kevin Harrington, and Erik Sahai. Fibroblast-led collective invasion of carcinoma cells with differing roles for RhoGTPases in leading and following cells. *Nature Cell Biology*, 9(12):1392–1400, 2007.

[5] P. Friedl, J. Locker, E. Sahai, and J. E. Segall. Classifying collective cancer cell invasion. *Nat. Cell Biol.*, 14(7):777–783, 2012.

[6] Vincent Hakim and Pascal Silberzan. Collective cell migration: a physics perspective. *Reports on Progress in Physics*, 80(7):076601, 2017.

[7] Duval K, Grover H, Han LH, Mou Y, Pegoraro AF, Fredberg J, and Chen Z. Modeling physiological events in 2d vs. 3d cell culture. *Physiology*, 32(4):266–277, 2017.

[8] A. A. Alobaidi and B. Sun. Probing three-dimensional collective cancer invasion with digme. *Cancer Convergence*, accepted, 2017.

[9] D. T. Tambe, C. C. Hardin, T. E. Angelini, K. Rajendran, C. Y. Park, X. Serra-Picamal, E. H. Zhou, M. H. Zaman, J. P. Butler, D. A. Weitz, J. J. Fredberg, and X. Trepat. Collective cell guidance by cooperative intercellular forces. *Nat. Mater.*, 10:469–475, 2011.

[10] J. Kim, J. Feng, C. A. R. Jones, X. Mao, L. M. Sander, H. Levine, and B. Sun. Stress-induced plasticity of dynamic biopolymer networks. *Nature Communications*, 2017, in press.

[11] C. A. Jones, L. Liang, D. Lin, Y. Jiao, and B. Sun. The spatial-temporal characteristics of type i collagen-based extracellular matrix. *Soft Matter*, 10(44):8855–8863, 2014.

[12] Hanqing Nan, Long Liang, Guo Chen, Liyu Liu, Ruchuan Liu, and Yang Jiao. Realizations of highly heterogeneous collagen networks via stochastic reconstruction for micromechanical analysis of tumor cell invasion. *Physical Review E*, 97(3):033311, 2018.

[13] J Steinwachs, C Metzner, K Skodzek, N.Lang, I Thievessen, C Mark, S Münster, K E Aifantis, and B Fabry. Three-dimensional force microscopy of cells in biopolymer networks. *Nat. Methods*, 13:171, 2016.

[14] S Chen, W Xu, J Kim, H Nan, Y Zheng, B Sun, and Y Jiao. Novel inverse finite-element formulation for reconstruction of relative local stiffness in heterogeneous extra-cellular matrix and traction forces on active cells. *Physical biology*, 16.

[15] L. Liang, C. AR. Jones, S. Chen, B. Sun, and Y. Jiao. Heterogeneous force network in 3d cellularized collagen networks. *Physical Biology*, 13:066001, 2016.

[16] Weijing Han, Shaohua Chen, Wei Yuan, Qihui Fan, Jianxiang Tian, Xiaochen Wang, Longqing Chen, Xixiang Zhang, Weili Wei, Ruchuan Liu, et al. Oriented collagen fibers direct tumor cell intravasation. *Proceedings of the National Academy of Sciences*, 113(40):11208–11213, 2016.

[17] Jingchen Feng, Herbert Levine, Xiaoming Mao, and Leonard M Sander. Stiffness sensing and cell motility: Durotaxis and contact guidance. *bioRxiv 320705*, 2018.

[18] Hanqing Nan, Yu Zheng, Yiheng H Lin, Shaohua Chen, Christopher Z Eddy, Jianxiang Tian, Wenxiang Xu, Bo Sun, and Yang Jiao. Absorbing–active transition in a multi-cellular system regulated by a dynamic force network. *Soft matter*, 15(35):6938–6945, 2019.

[19] Yu Zheng, Hanqing Nan, Qihui Fan, Xiaochen Wang, Liyu Liu, Ruchuan Liu, Fangfu Ye, Bo Sun, and Yang Jiao. Modeling cell migration regulated by cell-ecm micromechanical coupling. *Physical Review E*, 100:043303, 2019.

[20] Tianzhi Luo, Krithika Mohan, Pablo A. Iglesias, and Douglas N. Robinson. Molecular mechanisms of cellular mechanosensing. *Nature Materials*, 12:10641071, 2013.

[21] Eline Boghaert, Jason P Gleghorn, KangAe Lee, Nikolce Gjorevski, Derek C Radisky, and Celeste M Nelson. Host epithelial geometry regulates breast cancer cell invasiveness. *Proceedings of the National Academy of Sciences*, 109(48):19632–7, 2012.

[22] KJ Cheung, E Gabrielson, Z Werb, and AJ Ewald. Collective invasion in breast cancer requires a conserved basal epithelial program. *Cell*, 155(7):1639, 2013.

[23] Nicola Aceto, Aditya Bardia, David.T. Miyamoto, Maria.C. Donaldson, Ben.S. Wittner, Joel.A. Spencer, Min Yu, Adam Pely, Amanda Engstrom, Huili Zhu, Brian.W. Brannigan, Ravi Kapur, Shannon.L. Stott, Toshi Shioda, Sridhar Ramaswamy, David.T. Ting, Charles.P. Lin, Mehmet Toner, Daniel.A. Haber, and Shyamala Maheswaran. Circulating Tumor Cell Clusters Are Oligoclonal Precursors of Breast Cancer Metastasis. *Cell*, 158(5):1110–1122, 2014.

[24] Brian A Camley, Yunsong Zhang, Yanxiang Zhao, Bo Li, Eshel Ben-Jacob, Herbert Levine, and Wouter-Jan Rappel. Polarity mechanisms such as contact inhibition of locomotion regulate persistent rotational motion of mammalian cells on micropatterns. *Proceedings of the National Academy of Sciences*, 111(41):14770–5, 2014.

[25] Juliane Zimmermann, Brian A Camley, Wouter-Jan Rap-

pel, and Herbert Levine. Contact inhibition of locomotion determines cell-cell and cell-substrate forces in tissues. *Proceedings of the National Academy of Sciences*, 113(10):2660–5, 2016.

[26] Naoya Yamaguchi, Takeomi Mizutani, Kazushige Kawabata, and Hisashi Haga. Leader cells regulate collective cell migration via Rac activation in the downstream signaling of integrin β1 and PI3K. *Scientific Reports*, 5:1–8, 2015.

[27] Zachary S. Dean, Paul Elias, Nima Jamilpour, Urs Utzinger, and Pak Kin Wong. Probing 3D collective cancer invasion using double-stranded locked nucleic acid biosensors. *Analytical Chemistry*, 88(17):8902–8907, 2016.

[28] Amani A Alobaidi, Yaopengxiao Xu, Shaohua Chen, Yang Jiao, and Bo Sun. Probing cooperative force generation in collective cancer invasion. *Physical Biology*, 14(4):045005, jun 2017.

[29] Dapeng Bi, Jorge H Lopez, Jennifer M Schwarz, and M Lisa Manning. Energy barriers and cell migration in densely packed tissues. *Soft matter*, 10(12):1885–1890, 2014.

[30] Jin-Ah Park, Jae Hun Kim, Dapeng Bi, Jennifer A Mitchel, Nader Taheri Qazvini, Kelan Tantisira, Chan Young Park, Maureen McGill, Sae-Hoon Kim, Bomi Gweon, et al. Unjamming and cell shape in the asthmatic airway epithelium. *Nature materials*, 14(10):1040, 2015.

[31] Paolo P Provenzano, Kevin W Eliceiri, Jay M Campbell, David R Inman, John G White, and Patricia J Keely. Collagen reorganization at the tumor-stromal interface facilitates local invasion. *BMC Medicine*, 4(1):38, 2006.

[32] M W Conklin, J C Eickhoff, K M Riching, C A Pehlke, K W Eliceiri, P P Provenzano, A Friedl, and P J Keely. Aligned Collagen Is a Prognostic Signature for Survival in Human Breast Carcinoma. *Am. J. Path.*, 178(3):1221, 2011.

[33] Hervé Acloque, Meghan S Adams, Katherine Fishwick, Marianne Bronner-Fraser, and M Angela Nieto. Epithelial-mesenchymal transitions: the importance of changing cell state in development and disease. *The Journal of clinical investigation*, 119(6):1438–49, 2009.